とが確かめられた。今後は、他の因子とあわせて悪性度との関連を調べていく予定である。

G．研究発表

1. 論文発表

① Oida K, Matsuda A, Jung K, Xia Y, Jang H, Amagai Y, Ahn G, Nishikawa S, Ishizaka S, Jensen-Jarolim E, Matsuda H, and Tanaka A. Nuclear factor-κB plays a critical role in both intrinsic and acquired resistance against endocrine therapy in human breast cancer cells. Scientific Reports 2014 17;4:4057. doi: 10.1038/srep04057.

②Nishikawa S, Tanaka A, Matsuda A, Oida K, Jang H, Jung K, Amagai Y, Ahn G, Okamoto N, Ishizaka S, Matsuda H. A molecular targeting against nuclear factor-κB, as a chemotherapeutic approach for human malignant mesothelioma. Cancer Medicine 2014 3:416- 425. doi: 10.1002/cam4.202.

③Amagai Y, Tanaka A, Jung K, Matsuda A, Oida K, Nishikawa S, Jang H, Ishizaka S, Matsuda H. Production of stem cell factor in canine mast cell tumors. Research in Veterinary Science 2014 96: 124-126. doi: 10.1016/j.rvsc.2013.10.014.

④ Amagai Y, Tanaka A, Matsuda A, Jung K, Oida K, Nishikawa S, Jang H, Matsuda H. Heterogeneity of internal tandem duplications in the c-kit of dogs with multiple mast cell tumours. Journal of Small Animal Practice 2013, 54:377-380. doi: 10.1111/jsap.12069.

⑤ Amagai Y, Tanaka A, Matsuda A, Oida K, Jung K, Nishikawa S, Jang H, Ishizaka S, Matsuda H. Increased expression of the antiapoptotic protein MCL1 in canine mast cell tumors. Journal Veterinary Medical Science, 2013 75:971-974.

2. 学会発表

①Oida K, Nishikawa S, Tanaka A, Matsuda H. NF-kappa B, a new target molecule in treatment of mesothelioma. 18th World Congress on Advances in Oncology, 2013, Greek.

② Tanaka A, Matsuda A, Amagai Y, Matsuda H. The role of splicing factors in glucocorticoid sensitivity in neoplastic lymphocytes. 18th World Congress on Advances in Oncology, 2013, Greek

③雨貝陽介、田中あかね、松田浩珍、他. KIT細胞膜外ドメインの点変異による肥満細胞の腫瘍化. 第156回日本獣医学会学術集会, 岐阜

④Nishikawa S, Tanaka A, Matsuda H. NF-κB as a chemotherapeutic target molecule for human malignant mesothelioma. EAACI-WAO Congress 2013, Italy

⑤Tanaka A, Matsuda A, Matsuda H. Splicing regulation of glucocorticoid receptor isoforms in lymphocytes with glucocoriticoid resistance. EAACI-WAO Congress 2013, Italy

H．知的財産権の出願・登録状況

なし

III. 研究成果の刊行に関する一覧表

研究成果の刊行に関する一覧表

雑誌

発表者氏名	論文タイトル名	発表誌名	巻号	ページ	出版年
Sugai A, Sato H, Hagiwara K, Kozuka-Hata H, Oyama M, Yoneda M, Kai C.	Newly identified minor phosphorylation site threonine-279 of measles virus nucleoprotein is a prerequisite for nucleocapsid formation.	J Virol	88(2)	1140-9	2014
Sugai, A., Sato, M., Yoneda, M. and Kai, C.	Phosphorylation of Measles Virus Nucleoprotein Affects Viral Growth by Changing Gene Expression and Genomic RNA Stability.	J Virol	87(21)	11684-92	2013
Yoneda, M., Georges-Courbot, M-C., Ikeda, F., Ishii, M., Jacquot, F., Raoul, H., Sato, H. and Kai, C.	Recombinant Measles Virus Vaccine Expressing the Nipah Virus Glycoprotein Protects against Lethal Nipah Virus Challenge.	PLoS ONE	8(3)	e58414	2013
Sugiyama, T., Yoneda, M., Kuraishi, T., Hattori, S., Inoue, Y., Sato, H. and Kai, C.	Measles virus selectively blind to signaling lymphocyte activation molecule as a novel oncolytic virus for breast cancer treatment.	Gene Therapy	20	338-347	2013
Tsuji T, Nakamori M, Iwahashi M, Nakamura M, Ojima T, Iida T, Katsuda M, Haya ta K, Ino Y, Todo T, Yamaue H.	An armed oncolytic herpes simplex virus expressing thrombospondin-1 has an enhanced in vivo antitumor effect against human gastric cancer.	Int J Cancer	132 (2)	485-494	2013
Koyama-Nasu R, Nasu-Nishimura Y, Todo T, Ino Y, Saito N, Aburatani H, Funato K, Echizen K, Sugano H, Haruta R, Matsui M, Takahashi R, Manabe E, Oda T, Akiyama T.	The critical role of cyclin D2 in cell cycle progression and tumorigenicity of glioblastoma stem cells.	Oncogene	32 (33)	3840-3845	2013
Tanaka M, Tsuno NH, Fujii T, Todo T, Saito N, Takahashi K.	Human umbilical vein endothelial cell vaccine therapy in patients with recurrent glioblastoma.	Cancer Sci	104 (2)	200-205	2013

Shibui S, Narita Y, Mizusawa J, Beppu T, Ogasawara K, Sawamura Y, Kobayashi H, Nishikawa R, Mishima K, Muragaki Y, Maruyama T, Kuratsu J, Nakamura H, Kochi M, Minamida Y, Yamaki T, Kumabe T, Tominaga T, Kayama T, Sakurada K, Nagane M, Kobayashi K, Nakamura H, Ito T, Yazaki T, Sasaki H, Tanaka K, Takahashi H, Asai A, Todo T, Wakabayashi T, Takahashi J, Takano S, Fujimaki T, Sumi M, Miyakita Y, Nakazato Y, Sato A, Fukuda H, Nomura K	Randomized trial of chemoradiotherapy and adjuvant chemotherapy with nimustine (ACNU) versus nimustine plus procarbazine for newly diagnosed anaplastic astrocytoma and glioblastoma (JCOG0305).	Cancer Chemother Pharmacol	71 (2)	511-512	2013
Koyama-Nasu R, Hruta R, Nasu-Nishimura Y, Taniue K, Katou Y, Shirahige K, Todo T, Ino Y, Mukasa A, Saito N, Matsui M, Takahashi R, Hoshino-Okubo A, Sugano H, Manabe E, Funato K, Akiyama T.	The pleiotrophin-ALK axis is required for tumorigenicity ofglioblastoma stem cells.	Oncogene	33(17)	2236-44	2014
Echizen K, Nakada M, Hayashi T, K, Morishita Y, Hirano S, Terai K, Todo Todo T, Ino Y, Mukasa A, Takayanagi S, Ohtani R, Saito N, Akiyama T.	PCDH10 is required for the tumorigenicity of glioblastoma cells.	Biochem Biophys Res Commun	444(1)	13-18	2014
Takahashi N, Yamaguchi K, Ikenoue T, Fujii T, Furukawa Y.	Identification of two Wnt-responsive elements in the intron of RING Finger Protein 43 (RNF43) gene.	PLoS ONE	9	e86582	2014
Yamaguchi K, Rui Yamaguchi R, Takahashi N, Ikenoue T, Fujii T, Shinozaki M, Tsurita G, Hata K, Niida A, Imoto S, Miyano S, Nakamura Y, Furukawa Y.	Overexpression of cohesion establishment factor DSCC1 through E2F in colorectal cancer.	PLoS ONE	9	e85750	2014

Shigeyasu K, Tanakaya K, Nagasaka T, Aoki H,Fujiwara T, Sugano K, Ishikawa H, Yoshida T, Moriya Y, Furukawa Y, Goel A, Takeuchi H.	Early detection of metachronous bile duct cancer in Lynch syndrome: report of a case.	Surg Today	Jul 31	published online	2013
Hiramoto T, Ebihara Y, Mizoguchi Y, Nakamura K, Yamaguchi K, Ueno K, Michizuki S, Yamamoto S, Nagasaki M, Furukawa Y, Tani K, Nakauchi H, Kobayashi M, Tsuji K.	Wnt3a stimulates maturation of impaired neutrophils developed from severe congenital neutropenia patient-derived pluripotent stem cells.	Proc Natl Acad Sci USA	110(8)	3023-3028	2013
Mae H, Ooi J, Takahashi S, Kato S, Kawakita T, Ebihara Y, Tsuji K, Nagamura F, Echizen H, Tojo A.	Acute kidney injury after myeloablative cord blood transplantation in adults: the efficacy of strict monitoring of vancomycin serum trough concentrations.	Transplant Infect Dis	15	181-6	2013
Oida K, Matsuda A, Jung K, Xia Y,Jang H, Amagai Y, Ahn G, Nishikawa S,Ishizaka S, Jensen-Jarolim E, Matsuda H,and Tanaka A.	Nuclear factor-kB plays a critical role in both intrinsic and acquired resistance against endocrine therapy in human breast cancer cells.	Scientific Reports	17(4)	4057	2014
Nishikawa S, Tanaka A, Matsuda A, Oida K, Jang H, Jung K, Amagai Y, Ahn G,Okamoto N, Ishizaka S, Matsuda H.	A molecular targeting against nuclear factor-kB, as a chemotherapeutic approach for human malignant mesothelioma.	Cancer Medicine	3	416–425	2014
Amagai Y, Tanaka A, Jung K, Matsuda A,Oida K, Nishikawa S, Jang H, Ishizaka S, Matsuda H.	Production of stem cell factor in canine mast cell tumors.	Res Vet Sci	96	124-126	2014
Amagai Y, Tanaka A, Matsuda A, Jung K, Oida K, Nishikawa S, Jang H,Matsuda H.	Heterogeneity of internal tandem duplications in the c-kit of dogs with multiple mast cell tumours.	Journal of Small Animal Practice	54	377-380	2013
Amagai Y, Tanaka A, Matsuda A, Oida K, Jung K, Nishikawa S, Jang H, Ishizaka S, Matsuda H.	Increased expression of the antiapoptotic protein MCL1 in canine mast cell tumors.	J Vet Med Sci	75	971-974	2013

Ⅳ．研究成果の刊行物・別刷

JVI
Journals.ASM.org

Newly Identified Minor Phosphorylation Site Threonine-279 of Measles Virus Nucleoprotein Is a Prerequisite for Nucleocapsid Formation

Akihiro Sugai,[a] Hiroki Sato,[b] Kyoji Hagiwara,[b]* Hiroko Kozuka-Hata,[c] Masaaki Oyama,[c] Misako Yoneda,[b] Chieko Kai[a,b]

International Research Center for Infectious Diseases,[a] Laboratory Animal Research Center,[b] and Medical Proteomics Laboratory,[c] Institute of Medical Science, University of Tokyo, Minato-ku, Tokyo, Japan

Measles virus nucleoprotein is the most abundant viral protein and tightly encapsidates viral genomic RNA to support viral transcription and replication. Major phosphorylation sites of nucleoprotein include the serine residues at locations 479 and 510. Minor phosphorylation residues have yet to be identified, and their functions are poorly understood. In our present study, we identified nine putative phosphorylation sites by mass spectrometry and demonstrated that threonine residue 279 (T279) is functionally significant. Minigenome expression assays revealed that a mutation at the T279 site caused a loss of activity. Limited proteolysis and electron microscopy suggested that a T279A mutant lacked the ability to encapsidate viral RNA but was not denatured. Furthermore, dephosphorylation of the T279 site by alkaline phosphatase treatment caused deficiencies in nucleocapsid formation. Taken together, these results indicate that phosphorylation at T279 is a prerequisite for successful nucleocapsid formation.

Measles virus (MV), a member of the *Morbillivirus* genus in the *Paramyxoviridae* family, is an important human pathogen that causes disease characterized by fever, cough, coryza, conjunctivitis, and a maculopapular rash. Although the use of effective vaccines has decreased global mortality from measles, it remains a major cause of high mortality among children in developing countries (1–3). MV has a nonsegmented negative-stranded RNA genome containing six structural genes encoding nucleoprotein (N), phosphoprotein (P), matrix (M) protein, fusion (F) protein, hemagglutinin (H) protein, and large (L) protein (4), and the P gene produces two accessory proteins, known as V and C (5, 6). N proteins encapsidate viral genomic RNA to support viral transcription and replication by an RNA-dependent RNA polymerase (RdRp) L protein. The P protein is a multifunctional protein (7, 8) that assists with viral transcription and replication as a cofactor of the L protein (9, 10). The C and V accessory proteins suppress host immune responses (11, 12). The M protein helps virus assembly, and the F and H proteins are required for membrane fusion and binding to the host cellular receptor, respectively (13).

N protein is the most abundant viral protein in infected cells (14) and is mainly required for viral transcription and replication. N proteins tightly associate with the viral genome and antigenome to form an N-RNA complex with a herringbone-like structure (15, 16). N proteins associate with every 6 bases of the 15,894-nucleotide viral genome and fully cover the genome RNA (17). This tight encapsidation allows the viral genome to be resistant to RNases and small interfering RNAs (18, 19). Viral transcription and replication occur on the N-RNA complex in association with viral RdRp (vRdRp), composed of L and P proteins. This complex of N-RNA, P protein, and L protein is called the nucleocapsid (NC) and comprises 2,649 copies of the N protein, about 300 copies of the P protein, and about 20 to 30 copies of the L protein (20–22). Singly expressed N proteins associate with cellular RNA to form NC-like structures through a nonspecific association (23–25). vRdRp first transcribes the RNA genome, and viral structural genes are expressed. When a sufficient quantity of N proteins has accumulated, the function of vRdRp shifts from transcription to replication and the RNA genome is replicated exponentially (21). During the replication step, nascent growing viral RNA is immediately encapsidated by N protein and full-length viral antigenomic RNA (positive-sense strand) is produced and serves as a template for genome (negative-sense strand) replication (26).

We previously reported that the major phosphorylation sites of the MV N protein were S479 and S510 (27). Additionally, the functional significance of the major phosphorylation sites of N protein to the viral life cycle includes viral gene expression, viral genome RNA stability, and regulation of P-protein phosphorylation (28, 29). However, despite double mutation of the major phosphorylation sites of MV N protein, it was still phosphorylated, albeit to a lesser extent. The N-protein minor phosphorylation sites have not been identified and are poorly understood. In the present study, we predicted nine minor phosphorylation sites within the N protein by mass spectrometry (MS) analysis and investigated these putative phosphorylation sites. Furthermore, we identified a functionally indispensable minor phosphorylation site at threonine-279 (T279) and examined the role of threonine phosphorylation in viral reproduction.

MATERIALS AND METHODS

Cells, plasmids, and antibodies. Cos7, 293, 293T, and Vero cells were propagated in Dulbecco's modified Eagle's medium (DMEM; Sigma) supplemented with 5% fetal bovine serum (JRH Bioscience), 2 mM L-glutamine, 100 U/ml penicillin, and 0.1 mg/ml streptomycin at 37°C in 5%

Received 6 June 2013 Accepted 2 November 2013
Published ahead of print 6 November 2013
Address correspondence to Chieko Kai, ckai@ims.u-tokyo.ac.jp.
* Present address: Kyoji Hagiwara, Viral Infectious Diseases Research Unit, RIKEN, Wako, Saitama, Japan.

doi:10.1128/JVI.01718-13

CO_2. COBL cells were maintained in RPMI 1640 medium (Sigma) with the same supplements described above. pCAGGS mammalian expression vectors (30) encoding wild-type (wt) N, N mutants, and P-protein genes from the HL strain of MV (31) were prepared as described previously (27). The generation of a polyclonal anti-MV N antibody has also been described previously (27).

MALDI-TOF/TOF MS analysis. MV-infected COBL cells were lysed, and NC-associated N proteins were purified by cesium chloride (CsCl) gradient centrifugation as described below. The N protein was separated by SDS-PAGE and stained with Coomassie brilliant blue. The band corresponding to the N protein was excised from the gel and destained five times with 50 mM NH_4HCO_3 in 50% methanol. The N protein was then subjected to in-gel digestion with trypsin or V8 protease at 37°C for 16 h as previously described (27, 32). The digested peptides of N protein were separated by nanoflow liquid chromatography (LC; KYA Technologies Corporation) and analyzed by matrix-assisted laser desorption ionization–time of flight (MALDI-TOF)/TOF MS (4700 proteomics analyzer) as described previously (27). Detected peptides were identified by a database search using MASCOT, version 2.0 (Matrix Science).

Immunoprecipitation assay. Cos7, 279T, and Vero cells were transfected with plasmids containing wt N and N mutants. At 24 h posttransfection, 0.38 mCi/ml of ^{32}P (phosphorus-32 radionuclide; PerkinElmer) or 0.06 mCi/ml of ^{35}S (EasyTag Express protein labeling mix; PerkinElmer) was added to the medium, and the cells were incubated at 37°C for 24 h. Cells were harvested and lysed in lysis buffer consisting of 0.5 mM EDTA and 0.5% Triton X-100 in phosphate-buffered saline (PBS) supplemented with protease inhibitor cocktail (BD Biosciences) and PhosSTOP phosphatase inhibitor cocktail (Roche) for 1 h at 4°C, and cell debris was removed from the lysate by centrifugation. The lysate was incubated with protein A–Sepharose CL-4B beads (Amersham Biosciences) and anti-MV N polyclonal antibody for 16 h at 4°C. The beads were collected, washed 5 times with PBS, and suspended in 2× Laemmli's sample buffer. Component proteins were separated by SDS-PAGE, and radioactive proteins were detected using an imaging plate and phosphorimager (FLA-5100; Fujifilm).

Minigenome expression assay. Precise methods for the minigenome experiment were described previously (27, 28). Briefly, 293 cells in 24-well plates were transfected with N, P, and L protein expression plasmids using Lipofectamine LTX reagent (Invitrogen) and Plus reagent (Invitrogen). After 24 h, viral minigenomic RNA encoding the firefly luciferase gene was transfected with Lipofectamine 2000 reagent (Invitrogen). On the following day, cells were lysed in passive lysis buffer (Promega), and luciferase activity was measured using a PicaGene luminescence kit (Tokyo Ink Manufacturing) according to the manufacturer's instructions. Fluorescence intensity was detected by use of a MiniLumat LB 9506 luminometer (Berthold).

N-P protein binding assay. Cos7 cells were transfected with either wt N or mutant N protein (T279A) expression plasmids and a P protein expression plasmid using Lipofectamine LTX reagent and Plus reagent. On the following day, cells were labeled with ^{35}S (0.06 mCi/ml) at 37°C for 24 h. The cells were lysed, and the lysate was incubated with protein A–Sepharose CL-4B and anti-N-protein antibody. The precipitated proteins were separated by SDS-PAGE and detected with a phosphorimager (FLA-5100).

Indirect immunofluorescence assay. Cos7 cells were transfected with expression vectors for wt N, N-protein mutants (T279A, T279D, T279E, S479A/S510A, ST8A, and ST11A), and P protein using the FuGENE 6 transfection reagent according to the manufacturer's instructions. At 24 h posttransfection, cells were fixed and permeabilized with 3% paraformaldehyde-PBS and 0.5% Triton X-100–PBS, respectively. The cells were incubated with polyclonal anti-N-protein antibody and monoclonal anti-P-protein antibody, followed by incubation with a 1:2,000 dilution of an Alexa Fluor 488 $F(ab')_2$ fragment of goat anti-rabbit IgG (H+L) (Invitrogen) and an Alexa Fluor 568 $F(ab')_2$ fragment of goat anti-mouse IgG (H+L) (Invitrogen) supplemented with Hoechst 33342 (Cambrex Bio Science). Fluorescence was visualized by use of a confocal laser scanning microscope (Fluoview FV1000-D system; Olympus).

Nucleocapsid purification. Cos7 cells were transfected with the expression plasmid for N protein or its mutants using the FuGENE 6 transfection reagent (Roche Applied Science) according to the manufacturer's instructions. At 48 h posttransfection, cells were lysed in TNE buffer (10 mM Tris [pH 7.8], 150 mM NaCl, 1 mM EDTA) supplemented with 1% NP-40 and protease inhibitor cocktail at 4°C for 30 min. The lysate was layered onto 1.5 ml each of 25%, 30%, and 40% (wt/vol) CsCl gradients in TNE buffer and centrifuged in a Beckman Sw55Ti rotor for 2 h at 55,000 rpm. The fraction containing the nucleocapsid was diluted with TNE buffer and centrifuged at 55,000 rpm to precipitate the nucleocapsid, which was resolved in an appropriate volume of PBS.

Western blot analysis. Expression plasmids for wt N and T279A were transfected in Cos7 cells, and each cell lysate was subjected to Western blot analysis to detect the expression level of the N protein relative to that of an internal control, GAPDH (glyceraldehyde-3-phosphate dehydrogenase). The cell lysates were then separated by CsCl gradient centrifugation. The NC fraction was collected and further centrifuged to precipitate the NC-like particles. The yields of the NC-like particles were also visualized and quantified by Western blotting. Briefly, the lysate of N-protein-transfected cells and purified nucleocapsids were subjected to 10% SDS-PAGE, and the separated proteins were transferred onto an Immobilon-P transfer membrane (Millipore). The membrane was blocked with BlockACE reagent (DS Pharma Biomedical) and then incubated with anti-N polyclonal antibody for 1 h at 37°C. The membrane was washed five times with 0.05% Tween-PBS and incubated with a 1:2,000 dilution of polyclonal goat anti-rabbit horseradish peroxidase-conjugated immunoglobulins (Dako Cytomation) for 1 h at 37°C. Immunoreactive bands were detected using enhanced chemiluminescence Western blotting detection reagents (GE Healthcare). Scanning of the chemiluminescence was performed with a luminescent image analyzer (LAS-1000UV minisystem; Fujifilm).

Electron microscopy. Cos7 cells were transfected with wt N or N T279A expression plasmids using the Plus reagent and Lipofectamine LTX reagent, and self-assembled NC-like particles were purified at 2 days posttransfection. Preparation of the samples for electron microscopy was performed as previously described (27). Briefly, purified NC-like particles were spotted on a copper grid coated with collodion and incubated for 5 min at room temperature. The samples were then negative stained with 2% uranyl acetate and observed under an electron microscope (H7000; Hitachi).

Limited proteolysis. The purified NC fraction of wt N, N T279A, and heat-denatured (for 10 min at 95°C) wt N were equally divided into eight tubes, and each aliquot was subjected to 0, 0.1, 0.25, 0.5, 1.0, 2.5, 5.0, or 10.0 μg/ml of trypsin treatment for 1 h at 37°C. The reactions were stopped by adding SDS sample buffer and heating for 5 min at 95°C, and then the samples were subjected to SDS-PAGE. The proteolytic bands were detected by immunoblotting using anti-N polyclonal antibodies.

Bacterial alkaline phosphatase (BAP) treatment and NC fractionation. Cos7 cells in 6-cm dishes were transfected with expression plasmids for wt N, N T279A, and ST10A using the FuGENE 6 transfection reagent. At 24 h posttransfection, the nucleocapsids were purified by CsCl gradient centrifugation and dissolved in 200 mM Tris-HCl buffer (pH 8.0) supplemented with Complete EDTA-free protease inhibitor (Roche Diagnostics). Each sample was incubated with or without 1.5 units of BAP and PhosSTOP phosphatase inhibitor cocktail for 2 h at 65°C, and then 500 mM NaCl was added and the mixture was incubated for 1 h at 37°C. NC-like particles were separated by CsCl gradient centrifugation (0.6 ml of 30% [vol/vol] glycerol, 1.2 ml of 20% [wt/vol] CsCl, 1.4 ml of 30% [wt/vol] CsCl, and 1.4 ml of 40% [wt/vol] CsCl in TNE buffer) in a Beckman Sw55Ti rotor for 16 h at 36,000 rpm, and the gradients were divided into seven fractions. The N proteins contained in each fraction were immunoprecipitated with protein A–Sepharose CL-4B and anti-N polyclonal antibodies and were subjected to SDS-PAGE and Western blot analysis to quantify the N-protein levels.

FIG 1 Identification of the minor phosphorylation sites in the N protein by MS analysis. (A) Trypsin-digested peptides of N protein were separated by nanoflow LC and analyzed by MALDI-TOF/TOF MS. (B) Phosphorylated peptides from V8 protease-digested N proteins were selectively analyzed and identified by MALDI-TOF/TOF MS. The analyzed peptides were identified with a MASCOT (version 2.0) database search and are shown in red.

RESULTS

Identification of a minor phosphorylation site of MV N protein. Previously, we performed MALDI-TOF/TOF MS and electrospray ionization-quadrupole-TOF MS analysis of MV N protein and identified two major phosphorylation sites from the tryptic peptides of N protein purified from cells transfected with an N protein-expressing plasmid (27). However, we did not identify minor phosphorylation sites of the N protein from these tryptic peptides. Therefore, in this study, we reexamined minor phosphorylation of the N protein by MALDI-TOF/TOF MS analysis using trypsin-digested N protein derived from MV-infected cells. Additionally, we investigated minor phosphorylation using V8 protease-digested N protein. In the latter case, phosphorylated peptides were selectively detected and analyzed by MALDI-TOF/TOF MS. As a result, the peptides digested with trypsin or V8 protease covered 70.5% of the N-protein sequence (Fig. 1A and B), and nine putative phosphorylation sites were predicted: T279, S294, S295, S407, S418, T454, S456, S457, and S460. We further investigated these putative phosphorylation sites to identify sites responsible for the minor phosphorylation of N protein. We prepared alanine substitution mutants for each putative phosphorylation site of N protein and examined the phosphorylation levels of each putative phosphorylation site by ^{32}P labeling and immunoprecipitation. The mutants used in this study are shown in Fig. 2A. As a result, among these nine putative phosphorylation sites, the T279 site was found to be remarkably phosphorylated, with a phosphorylation rate of 14.3% for wt N protein in Cos7 cells (Fig. 2B). We also investigated the phosphorylation rate of T279 in Vero and 293T cells but did not observe a significant change in the rate in these cells compared with that in Cos7 cells (Fig. 2C). This indicated that the minor phosphorylation at T279 was not a cell-type-specific phenomenon. Phosphorylation at the eight remaining putative phosphorylation sites occurred at trace levels, and therefore, these sites may not be phosphate group acceptors. Additionally, phosphorylation signals were barely detected in the ST11A mutant, where two major and nine minor putative phosphorylation sites had alanine substitutions.

The *Paramyxovirus* N protein possesses a highly conserved domain at amino acids (aa) 258 to 357 which is referred to as the central conserved region (CCR) (Fig. 2D) and is known to be important for N-protein function (33, 34). In a previous analysis (27) and the present MS analysis (Fig. 1), aa 250 to 278 and 298 to 324 were not covered within the N-protein CCR. This region includes six serine and threonine residues: T259, S268, T272, S298, T309, and S319. We generated additional alanine mutants, the ST14A and ST17A mutants (Fig. 2E), and examined whether the low phosphorylation levels detected in the ST11A mutant was the result of phosphorylation of these sites. The level of phosphorylation of the ST14A and ST17A mutants was similar to that of the ST11A mutant (Fig. 2F), suggesting that these six sites within CCR are not phosphate group acceptors. The trace levels of phosphorylation detected in the ST11A, ST14A, and ST17A mutants appeared to be because of nonspecific phosphorylation that occurred at very low rates.

T279 is an indispensable phosphorylation site for N-protein function. To identify the phosphorylation sites required for N-protein function from the nine putative sites, we prepared alanine-substituted mutants of N protein and measured the N-protein activity of each one by a minigenome reporter assay. In agreement with our previous reports, a mutant with mutations of both major phosphorylation sites, S479A and S510A, showed 46.3% activity compared with that for the wt N protein (Fig. 3A), whereas an alanine substitution mutant with a mutation of the T279 site showed a complete loss of activity and the N protein did not aid transcription and replication, indicating that the T279 site is functionally important. A mutant N protein with alanine substitution mutations at the eight putative phosphorylation sites other than T279 (the ST8A mutant) showed no reduction in activity compared with that of wt N protein. Additionally, the activity of the ST10A mutant (where the amino acids at two major phosphorylation sites and eight putative phosphorylation sites other than T279 were replaced by alanine) was reduced to 36.6% of that of wt N protein. There was no statistically significant difference between the activities of the S479A/S510A and ST10A mutants. Thus, the eight putative phosphorylation sites other than T279 were not required for N-protein function, but the T279 site was found to be functionally indispensable. Therefore, we investigated the T279 site further using N-protein mutants with aspartic acid (D) and glutamic acid (E) substitutions at the T279 site. The T279D and T279E mutants showed no activity, similar to the result for the T279A mutant, in the minigenome assay (Fig. 3B). Since the replacement of T279 with acidic residues did not mimic the phosphorylation of T279, constitutively charged T279 may be undesirable for N-protein function.

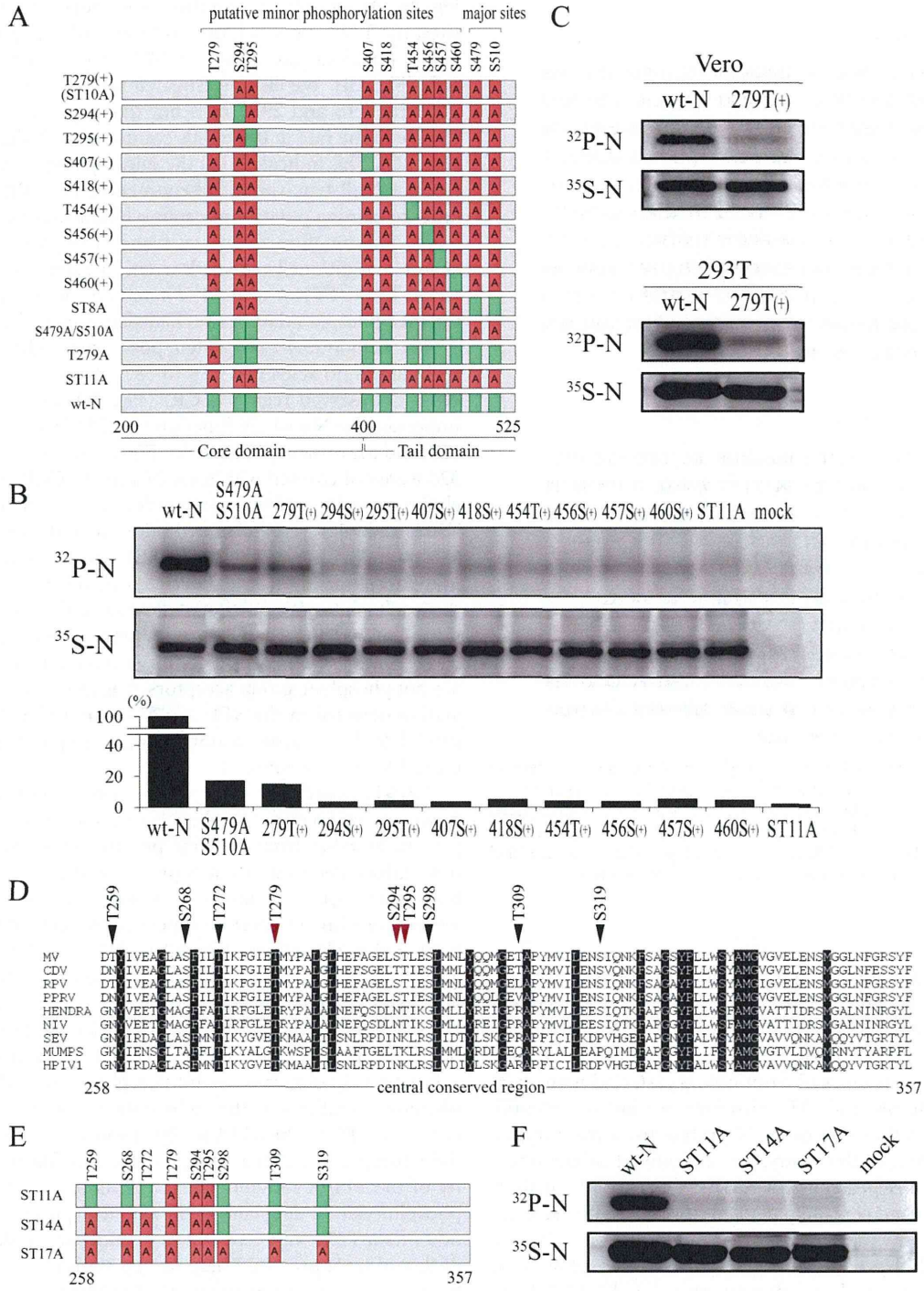

FIG 2 Analysis of minor phosphorylation sites of N protein. (A) Schematic diagram of the alanine substitution mutants of the N protein used in this study. Each phosphorylation site is indicated as a green square, and sites where the amino acid was with an alanine residue are shown as red squares with a letter A. (B) Identification of the minor phosphorylation site in the N protein by immunoprecipitation assay. The N protein or its phosphorylation mutants were radiolabeled with ^{32}P or ^{35}S in Cos7 cells. The relative phosphorylation (^{32}P-N/^{35}S-N) of each N protein mutant was quantified. (C) Phosphorylation of wt N and the T279A mutant in 293T and Vero cells. (D) Multiple-sequence alignment of the N protein CCR (aa 258 to 357) from *Paramyxoviruses*: canine distemper virus (CDV; GenBank accession no. AAG30916), rinderpest virus (RPV; CAA48388), peste des petits ruminants virus (PPRV; ACN62116), Hendra virus (AAC83187), Nipah virus (NIV; AAK50548), Sendai virus (SEV; AAB06278), mumps virus (CBA10117), and human parainfluenza virus type 1 (HPIV1; NP_604433). Black and red arrowheads, S or T residues untested by MS analysis and putative phosphorylation sites detected by MS analysis, respectively. (E) Schematic diagram of additional mutants with mutations at the CCR. (F) Phosphorylation properties of the mutants.